

## Poly(lactide)-Grafted Dextrans: Synthesis and Properties at Interfaces and in Solution

Cécile Nouvel,<sup>†</sup> Céline Frochot,<sup>‡</sup> Véronique Sadtler,<sup>§</sup> Philippe Dubois,<sup>||</sup> Edith Dellacherie,<sup>†</sup> and Jean-Luc Six<sup>\*,†</sup>

Laboratoire de Chimie-Physique Macromoléculaire, UMR CNRS-INPL 7568, Groupe ENSIC, 1 rue Grandville, B.P. 451, 54000 Nancy, France, Département de Chimie Physique des Réactions, UMR 7630 CNRS–INPL, Groupe ENSIC, 1 rue Grandville, B.P. 451, 54000 Nancy, France, Centre de Génie Chimique des Milieux Rhéologiquement Complexes, EA 1743, Groupe ENSIC, 1 rue Grandville, B.P. 451, 54000 Nancy, France, and Laboratory of Polymeric and Composite Materials, University of Mons-Hainaut, Place du Parc 20, B-7000 Mons, Belgium

Received January 21, 2004; Revised Manuscript Received April 23, 2004

**ABSTRACT:** A large variety of amphiphilic poly(lactide)-grafted dextrans has been synthesized with controlled architecture through a three-step procedure: partial protection of the dextran hydroxyl groups by silylation; ring-opening polymerization of D,L-lactide initiated from remaining hydroxyl groups on partially silylated dextran; and silyl ether deprotection under very mild conditions. Throughout the synthesis, detailed characterizations of each step led to the control of copolymer architecture in terms of graft number and lengths of graft and backbone. Depending on their proportion in poly(lactide), these copolymers were either water-soluble or soluble in organic solvents. The potential of these amphiphilic grafted copolymers as surfactants was estimated. Their organization at air/water or dichloromethane/water interfaces was investigated by interfacial tension measurements. Self-organization in water or toluene was evaluated using fluorescence spectroscopy. Depending on its solubility, each copolymer showed noticeable surfactant properties and was able to produce either hydrophobic or hydrated microdomains in water or toluene solutions, respectively.

### Introduction

With increasing environmental concerns, several researches have recently focused on nontoxic or biodegradable surfactants. For ecological purposes, polysaccharide-based materials (glycopolymers) are interesting mainly because polysaccharides are obtained from renewable resources and are easily degraded.

However, in case of amphiphilic glycopolymers, their associative properties in semidilute aqueous solution<sup>1–6</sup> have more often been studied than their organization in dilute solution<sup>7</sup> or their surfactant properties.<sup>8–11</sup> The interest for this latest point has progressively grown in recent years and most of the reports dealing with surfactant potentiality concern either hydrophobized polysaccharides or oligosaccharide-based surfactants. To the best of our knowledge, the surfactant properties of totally biodegradable polysaccharide-based copolymers such as polyester-grafted dextrans have not been published, even though they have been recently used for the formulation of nanoparticles used as drug delivery vehicles.<sup>12</sup> Besides, polyester-grafted polysaccharides present nowadays an attractive research field as they can be used as blend compatibilizer<sup>13–15</sup> or for biomedical applications<sup>3,12,16,17</sup> when they are totally biodegradable.

Various authors have reported the attempts to control the synthesis of such polyester-grafted glycopolymers but none of them has ever achieved either a real control

of the copolymer architecture or a broad range of copolymer compositions.<sup>3,12–17</sup> In some of these reports, lactic acid or  $\epsilon$ -caprolactone oligomers were grafted onto polysaccharide backbone. In some others, polyester-grafted polysaccharides have been synthesized thanks to the “grafting from” strategy, either by polycondensation of lactic acid<sup>3,14</sup> or by ring-opening polymerization (ROP) of  $\epsilon$ -caprolactone<sup>13,18–20</sup> or D,L-lactide (lactic acid dimer)<sup>15–17,21</sup> but without control of the synthesis.

A few years ago, some of us reported on the controlled synthesis of amphiphilic polyester-grafted polysaccharides by associating dextran with poly( $\epsilon$ -caprolactone).<sup>22</sup> Then, the synthetic scheme was recently extended to the synthesis of poly(lactide)-grafted dextran (Dex-*g*-PLA).<sup>23–25</sup> The control over the macromolecular parameters of such grafted copolymers required a three-step strategy based on the “grafting from” concept, as shown in Scheme 1. In a first step, most of the dextran hydroxyl functions were protected by a controlled silylation to get solubility in solvents usually used for the ROP of lactide and to allow polymerization in homogeneous medium. On the basis of the “grafting from” strategy, grafts were generated by ROP of D,L-lactide in toluene from the free remaining hydroxyl groups of the partially silylated dextran. To control the ROP, a catalytic amount of SnOct<sub>2</sub> was used to enhance the rate of propagation with regard to that of transesterification reactions.<sup>23</sup> In the third and final step, silyl ether deprotection led to the amphiphilic poly(lactide)-grafted dextran. As previous articles<sup>23–25</sup> have already paved the way for the macromolecular control, this paper will be focused on the self-organization properties of the amphiphilic poly(lactide)-grafted dextran copolymers. First, a brief description of the synthesis, macromolecular parameters, and solubility properties of such copolymers will be resumed. Then, in the main part of this paper, we will report both

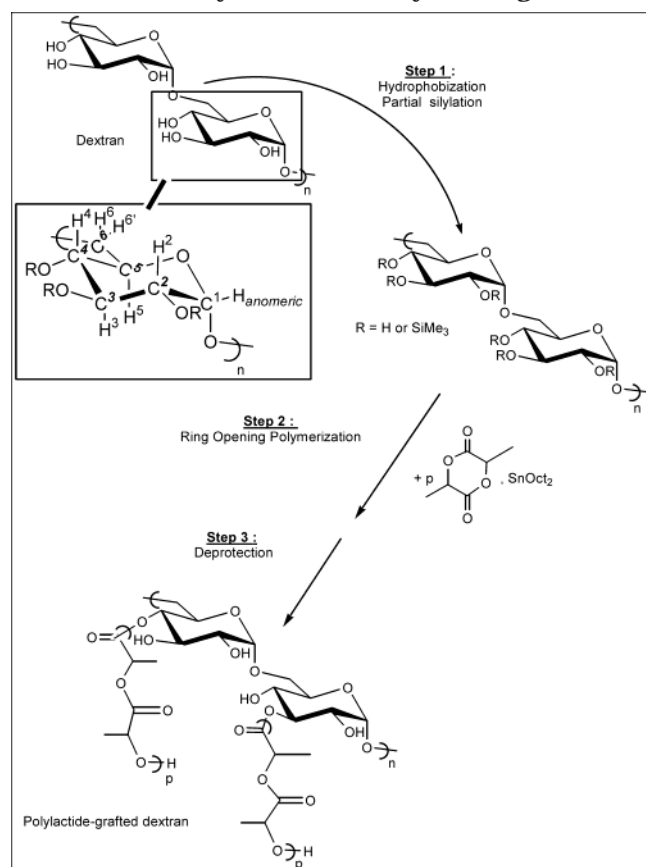
\* Corresponding author. Tel: 33(0)3-83-17-52-61; fax: 33(0)3-83-37-99-77; e-mail: Jean-Luc.Six@ensic.inpl-nancy.fr.

<sup>†</sup> Laboratoire de Chimie-Physique Macromoléculaire.

<sup>‡</sup> Département de Chimie Physique des Réactions.

<sup>§</sup> Centre de Génie Chimique des Milieux Rhéologiquement Complexes.

<sup>||</sup> University of Mons-Hainaut.

Scheme 1. Synthetic Pathway to Dex-*g*-PLA

the adsorption at interfaces and the self-organization in solution of these copolymers from interfacial tension and fluorescence spectroscopy measurements, respectively.

## Experimental PART

**2.1 Materials.** Dextran T40 ( $\overline{M}_n = 29\,000\text{ g mol}^{-1}$  and  $I = 1.3$ ) was purchased from Pharmacia Biotech and dried under reduced pressure at  $100\text{ }^\circ\text{C}$  for one night. Stannous octoate ( $\text{SnOct}_2$ ) was purchased from Aldrich and used without any further purification. After dilution in dry toluene,  $\text{SnOct}_2$  solution was stored in glass ampules under nitrogen. D,L-Lactide from Lancaster was recrystallized twice with dry toluene and dried under vacuum before use. Toluene and dimethyl sulfoxide (DMSO) were dried over polystyryllithium and  $\text{CaH}_2$ , respectively, and were distilled.

**2.2 Dex-*g*-PLA<sub>m</sub> Synthesis.** The whole controlled synthesis of Dex-*g*-PLA was performed as previously described.<sup>23–25</sup> In the following text, the symbol Dex-*g*-PLA<sub>m</sub> is used to design PLA-grafted dextrans.  $n$  (in g/mol) is the  $\overline{M}_n$  of the dextran backbone (determined after deprotection of silylated dextran under mild conditions)<sup>25</sup>;  $m$  (in g/mol) is the  $\overline{M}_n$  of PLA grafts ( $\overline{M}_{n,\text{graft}}$ ), and  $y$  is the average number of PLA grafts per 100 glucose units.

**Dextran Silylation.** Silylation yields ( $t$ ) were calculated using  $^1\text{H}$  NMR spectrum ( $\text{CDCl}_3$ ) of partially silylated dextrans by comparison of  $A_{\text{OSiMe}_3}$  and  $A_{\text{anomericH}}$  which are the respective areas of the trimethylsilyl group (at  $0.15\text{ ppm}$  in  $\text{CDCl}_3$ ) and of the anomeric protons centered at  $4.7\text{ ppm}$  in  $\text{CDCl}_3$  (eq 1):

$$t(\%) = \frac{A_{\text{OSiMe}_3}}{A_{\text{anomericH}}} \times \frac{100}{27} \quad (1)$$

**ROP of D,L-Lactide from Silylated Dextran.** As previously described,<sup>23</sup> a dried partially silylated dextran was dissolved in dry toluene. A defined volume of  $\text{SnOct}_2$  was then

added to the resulting solution at  $80\text{ }^\circ\text{C}$ . This mixture was then transferred to a hot D,L-lactide toluene solution. Polymerization temperature was kept at  $100\text{ }^\circ\text{C}$  for 20 h. After the polymerization was stopped by addition of a catalytic amount of acidic methanol, the D,L-lactide conversion was determined by  $^1\text{H}$  NMR analysis of the crude product in  $\text{CDCl}_3$ .<sup>23</sup> The pure product was recovered by precipitation, filtration, and dried under vacuum. Poly(lactide)-grafted (silylated dextran) was analyzed afterward by  $^1\text{H}$  NMR in  $\text{CDCl}_3$ . The silylation yields thus estimated were similar to those observed before the polymerization step. Considering that all the free hydroxyl groups carried by the partially silylated dextran exhibited the same reactivity and initiated the polymerization of the D,L-lactide (because of the rapid equilibrium between free OH and tin alkoxides *in situ* produced by reaction between OH and  $\text{SnOct}_2$ ), the  $\overline{DP}_n$  of PLA grafts ( $\overline{DP}_{n,\text{graft}}$ ) could be estimated by eq 2:

$$\overline{DP}_{n,\text{graft}} = \frac{A_{\text{CHPLA}}}{A_{\text{glucosidic}}} \times \frac{1}{\left(1 - \frac{t}{100}\right)} \quad (2)$$

where  $A_{\text{glucosidic}}$  and  $A_{\text{CHPLA}}$  are, respectively, the areas of glucosidic protons (from  $3.0$  to  $4.0\text{ ppm}$ ) and methyne protons of poly(lactide) (from  $5.15$  to  $5.4\text{ ppm}$ ).  $t$  is the silylation yield of the partially silylated dextran (in percent).

The number of PLA grafts ( $y$ ) per 100 glucose units could be estimated by eq 3.

$$y = 3\left(1 - \frac{t}{100}\right) \times 100 \quad (3)$$

**Deprotection of the Poly(lactide)-Grafted (Silylated Dextran).** The silylated grafted copolymers were dissolved in THF and  $0.02\text{ mol}$  of  $\text{HCl}$  ( $0.1\text{ M}$ ) per mol of  $\text{OSiMe}_3$  was added afterward. After 2 h at room temperature, the deprotected copolymers (PLA-grafted dextran) were recovered by precipitation from ethanol and then dried overnight at  $50\text{ }^\circ\text{C}$  under vacuum. These copolymers were analyzed by  $^1\text{H}$  NMR in  $d_6$ -DMSO and their PLA weight fraction ( $F^{\text{PLA}}$ ) was evaluated from eq 4, where  $M_{\text{GU}}$  is the molar mass of a glucosidic unit:

$$F^{\text{PLA}} = \frac{A_{\text{CHPLA}} \times 72}{A_{\text{CHPLA}} \times 72 + \frac{A_{\text{glucosidic}}}{6} \times M_{\text{GU}}} \quad (4)$$

**2.3 Interfacial Tension Measurements.** Surface (water/air) and interface (dichloromethane/water) tension measurements were carried out at  $25\text{ }^\circ\text{C}$  using a K8 surface tensiometer (Krüss, Germany).

In water-soluble copolymers, solutions were prepared with ultrapure water (Milli Q water purification system, Millipore) and then allowed to stand overnight at  $4\text{ }^\circ\text{C}$  before measurement. Surface tension was measured at air/water interface using the Wilhelmy technique. All samples were equilibrated for a sufficient time to reach constant readings.

Dichloromethane solutions of copolymers soluble in organic solvents were prepared using freshly distilled dichloromethane, stored in the dark, and allowed to stand overnight at  $4\text{ }^\circ\text{C}$ . Afterward, interfaces were prepared by adding slowly water on dichloromethane solution and were further equilibrated for 24 h to reach constant readings before measurements. Interfacial tension was determined with a platinum ring at water/dichloromethane solution interface (Lecomte de Noüy method). The Harkins/Jordan correction was applied.<sup>26</sup> In each case, the experimental errors were in the  $0.2\text{ mN/m}$  range.

**2.4 Fluorescence Measurements.** Pyrene (Figure 1) was purchased from the Community Bureau of Reference-Bruxelles ( $n^\circ 177$ ) and 1-anilinonaphthalene-8-sulfonic acid (ANS, Figure 1) was supplied by Molecular Probes-Leiden, The Netherlands. As already reported,<sup>27</sup> ANS exists in two different geometrical conformations: planar and nonplanar (Figure 1). The molecular

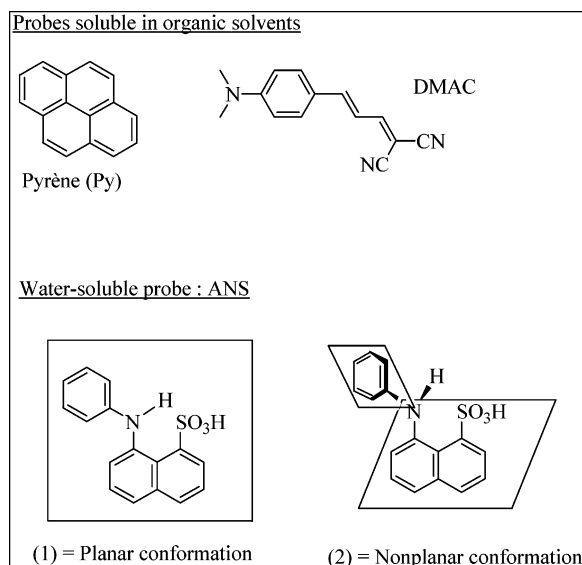


**Figure 1.** Chemical structure of the various molecular probes used in this study.

rotor 1,1-dicyano-4-(*N,N*-dimethylaminophenyl)-1,3-butadiene (DMAC, Figure 1) was synthesized as previously described.<sup>28</sup>

Fluorescence emission spectra were recorded on a Spex-fluorolog-2 spectrometer equipped with a thermostated cell compartment at 25 °C (slit width = 0.5 mm,  $\Delta\lambda_{1/2}$  = 2 nm). Before each experiment, fluorescence emission spectra of a reference solution (fluorescein at 0.16 mg/L in water) were recorded with  $\lambda_{\text{ex}}$  = 473 nm ( $\lambda_{\text{ex}}$  = excitation wavelength) and the intensity was measured at  $\lambda_{\text{em}}$  = 512 nm ( $\lambda_{\text{em}}$  = emission wavelength). In addition, the absence of noticeable fluorescence emission of the pure polymer solutions was verified.

**Water-Soluble Copolymers.** Stock solutions of water-soluble Dex-*g*-PLA (concentration above 0.5 g/L) were prepared with ultrapure water (Milli-Q water purification system, Millipore). They were left under vigorous stirring for 24 h and stored at 4 °C. Before measurements, the fluorescent probe was added and solutions were stirred again to ensure the complete incorporation of the fluorescent probe in the hydrophobic microdomains.

At the concentration of pyrene used ( $1.1 \times 10^{-6}$  mol/L), no excimer band was observed. All samples were excited at  $\lambda_{\text{ex}}$  = 330 nm and the fluorescence emission spectrum of pyrene was registered in the range 350–500 nm. Specific vibronic peaks were observed at  $\lambda_1$  = 372 nm (intensity  $I_1$ ) and  $\lambda_3$  = 383 nm (intensity  $I_3$ ).

Regarding DMAC ( $3.3 \times 10^{-6}$  mol/L), all samples were excited at  $\lambda_{\text{ex}}$  = 493 nm and the emission spectra were registered in the range 510–700 nm. In all cases, the excitation generated one single fluorescence peak, whose maximum wavelength ( $\lambda_{\text{max}}$ ) was medium-dependent. Both intensity ( $I_{\text{max}}$ ) of this peak and  $\lambda_{\text{max}}$  were compared to a reference solution containing only DMAC, without any copolymer. Thus, the fluorescence quantum yield ratio ( $\Phi_f/\Phi_0$ , where  $\Phi_f$  and  $\Phi_0$  are the fluorescence quantum yield, respectively, with and without amphiphilic copolymer) were estimated.

**Copolymers Soluble in Organic Solvents.** The applied protocol was similar to that of Vasilescu's method.<sup>27</sup> ANS probe stock solution ( $2.5 \times 10^{-3}$  mol/L) was prepared with absolute ethanol (spectrophotometric quality). Besides, a stock solution of PLA-grafted dextran (5 g/L) was prepared in toluene (spectrophotometric quality, purity >9.5%, and [H<sub>2</sub>O] < 0.3%) and was stirred for 24 h at 25 °C. Then, an adequate amount of the probe stock solution was introduced into a flask; ethanol was thoroughly evaporated for 1 h in the dark and a known amount of the stock copolymer solution was then put into this vial to ensure a final ANS concentration of  $2.8 \times 10^{-6}$  mol/L. The solution thus obtained (A) was homogenized by stirring for 1 h. Ultrapure water was then added to a fraction of this solution (A) to lead to another stock solution (B) with the maximum

**Table 1.** Macromolecular Parameters of Dex-*g*-yPLA<sub>m</sub><sup>c</sup>

entry	copolymers	$\overline{M}_n$ (g/mol) <sup>a</sup>	y <sup>b</sup>	$\overline{M}_{n \text{ graft}}$ (g/mol) <sup>c</sup>	F <sup>PLA</sup> <sup>d</sup>
1	Dex <sub>13K</sub> - <i>g</i> - <sub>27</sub> PLA <sub>0.4K</sub>	13 000	27	360	0.37
2	Dex <sub>13K</sub> - <i>g</i> - <sub>39</sub> PLA <sub>0.9K</sub>	13 000	39	940	0.69
3	Dex <sub>13K</sub> - <i>g</i> - <sub>27</sub> PLA <sub>2.5K</sub>	13 000	27	2 500	0.81
4	Dex <sub>29K</sub> - <i>g</i> - <sub>18</sub> PLA <sub>0.1K</sub>	28 900	18	100	0.10
5	Dex <sub>29K</sub> - <i>g</i> - <sub>14</sub> PLA <sub>0.2K</sub>	28 900	14	200	0.15
6	Dex <sub>29K</sub> - <i>g</i> - <sub>18</sub> PLA <sub>1.7K</sub>	28 900	18	1 700	0.66
7	Dex <sub>29K</sub> - <i>g</i> - <sub>60</sub> PLA <sub>2.0K</sub>	28 900	60	2 000	0.88

<sup>a</sup>  $\overline{M}_n$  of dextran backbone determined after deprotection of partially silylated dextran<sup>25</sup> under mild conditions. <sup>b</sup> Average number of PLA grafts per 100 glucose units, calculated from eq 3.

<sup>c</sup> Calculated from  $\overline{M}_{n \text{ graft}} = 144 \times \overline{\text{DP}}_{n \text{ graft}} \cdot \overline{\text{DP}}_{n \text{ graft}}$  was evaluated from eq 2.<sup>23</sup> <sup>d</sup> PLA weight fraction calculated from eq 4. <sup>e</sup>  $n$  (in g/mol) is the  $\overline{M}_n$  of the dextran backbone,  $m$  (in g/mol) is the ( $\overline{M}_{n \text{ graft}}$ ), and  $y$  is the average number of PLA grafts per 100 glucose units.

water concentration required for the experiments. Different proportions of solutions (A) and (B) were mixed to produce final solutions with different amounts of water (expressed in mg/mL). After 30 min stirring, solutions were left overnight to ensure a total homogenization.

Measurements were performed in 1-cm-length quartz cells. All samples were excited at  $\lambda_{\text{ex}}$  = 375 nm and the emission spectrum of ANS was registered in the range 400–600 nm. In all cases, the excitation generated one single fluorescence peak whose maximum wavelength ( $\lambda_{\text{max}}$ ) was medium-dependent. Then, this single peak was deconvoluted into two Gaussian bands,<sup>27</sup> which are characteristic of the two ANS conformations. Each band was characterized by its area ( $A_1$  and  $A_2$ ) and its wavelength ( $\lambda_1$  and  $\lambda_2$ ).

## Results and Discussion

**3.1 Synthesis, Characteristics, and Solubility of Dex-*g*-yPLA<sub>m</sub>.** According to the previous detailed studies,<sup>22,24,25</sup> different Dex-*g*-PLA<sup>23</sup> were designed with various macromolecular parameters such as PLA weight fraction ( $F^{\text{PLA}}$ ), average number of PLA grafts per 100 glucose units ( $y$ ), graft position onto the backbone, and lengths of both backbone and grafts. The macromolecular parameters of some selected copolymers are shown in Table 1. The three-step strategy used for this synthesis is described in Scheme 1.

Hydrophobization of dextran was achieved by a controlled silylation reaction, that is, leading to a partially silylated polysaccharide with a low number of residual free OH functions, potentially available for further ROP of D,L-lactide. It was shown that high silylation yields could be achieved without any degradation of the polysaccharide backbone.<sup>23</sup> However, it was observed that some experimental conditions could induce a degradation, that is, the reduction of the polysaccharide molecular weight. This is the reason why the copolymers reported in Table 1 are characterized by two different molecular weights of dextran backbone ( $\overline{M}_n$  = 29 000 and 13 000 g/mol); the second value is the result of the aforementioned dextran degradation. In this first step, the average number of residual OH functions along the dextran chain, as well as the average number ( $y$ ) of PLA grafts per 100 glucose units, could be modulated in a controlled manner (Table 1). In this study,  $y$  varied in a wide range from 14 to 60. Besides, the reactivity of the different dextran OH functions toward silylation has also been examined. For high silylation yields, the remaining OH groups were located mainly on the third carbon (C<sup>3</sup>) of glucose units and, to a least extent, on the fourth carbon (C<sup>4</sup>) (Scheme 1).<sup>25</sup> Consequently, it



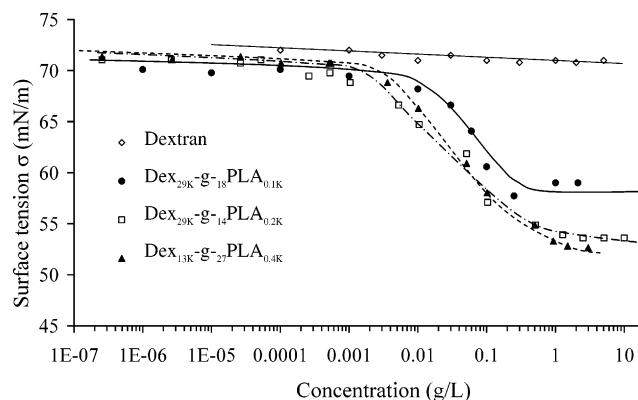


**Figure 2.** Variation of the surface tension ( $\sigma$ ) of aqueous polymer solutions (dextran or water-soluble Dex-*g*-PLA) versus polymer concentration at 25 °C.

could be assumed that the PLA grafts were located on these positions.

In the second step, the partially silylated dextran was used as a multifunctional macroinitiator for the ROP of D,L-lactide in the presence of a low amount of tin activator ( $\text{SnOct}_2$ ).<sup>23</sup> All the results obtained by NMR as well as SEC have demonstrated both the efficiency of the polylactide grafting onto the silylated dextran backbone and the absence of significant transesterification.

Different conditions were previously tested<sup>23</sup> to deprotect the silyl ether groups but, to avoid backbone and graft degradations, this deprotection was performed under very mild acidic conditions. Besides, one can see from Table 1 that copolymers with very different polylactide weight fractions ( $F^{\text{PLA}}$ ) from 0.10 up to around 0.9 could be synthesized. Depending on this polylactide/dextran ratio, the PLA-grafted dextran copolymers exhibited different solubility characteristics: those with high dextran/PLA ratios were water-soluble (Table 1, entries 1, 4, 5) whereas those with high  $F^{\text{PLA}}$  were soluble in organic solvents (Table 1, entries 2, 3, 6, 7). In a previous paper,<sup>23</sup> we rapidly mentioned that these copolymers were able to adapt their conformation to be soluble in various solvents. Thus, when  $^1\text{H}$  NMR spectra were recorded in  $d_6$ -DMSO, which can solubilize both parts of the copolymer, the PLA weight fraction of the copolymers ( $F^{\text{PLA}}$ ) was in good agreement with the theoretical value. However, in other deuterated solvents, only one part of the copolymer (PLA or dextran) appeared in the NMR spectra. A core-shell conformation whose structure depended on the solubility of copolymers in the studied solvents was thus proposed.

**3.2 Behavior of Dex-*g*-PLA<sub>m</sub> at Interfaces.** Whatever the solubility of the copolymers, their properties were studied at interfaces via tension measurements. Depending on their solubility, the interfacial properties were studied either by steady-state surface tension at air/water interface (water-soluble copolymers) or by interfacial tension measurements at water/organic solvent interface (copolymers soluble in organic solvents).

**Water-Soluble Copolymers.** Figure 2 highlights the influence of the different water-soluble Dex-*g*-PLA on the steady-state surface tension ( $\sigma$ ) of water as a function of the copolymer concentration ( $C$  between  $10^{-7}$  and 10 g/L). All copolymers exhibit relatively similar surface tension properties. Furthermore,  $\sigma$  versus  $\log C$  plots are similar to those of conventional nonionic molecular surfactants where a sharp inflection point is observed at the CMC. In Figure 2, it can be seen that  $\sigma$

**Table 2.** Comparison of the Various Critical Aggregation Concentrations (CAC in g/L) Obtained from Fluorescence Experiments with Pyrene or DMAC or from Steady-State Surface Tension

copolymer	CAC <sub>polarity</sub> from		CAC <sub>cohesion</sub> from ( $\Phi_f/\Phi_0$ ) <sup>b</sup>	CAC <sup>c</sup>
	$I_1/I_3$ <sup>a</sup>	$\lambda_{\text{max}}$ <sup>b</sup>		
Dex29K- <i>g</i> -18PLA <sub>0.1K</sub>	$1.5 \cdot 10^{-2}$	$3.0 \cdot 10^{-2}$	$9.0 \cdot 10^{-2}$	0.30
Dex29K- <i>g</i> -13.5PLA <sub>0.2K</sub>	$2.0 \cdot 10^{-2}$	$4.0 \cdot 10^{-2}$	$7.0 \cdot 10^{-2}$	0.55

<sup>a</sup> From fluorescence experiments carried out with pyrene.

<sup>b</sup> From fluorescence experiments carried out with DMAC. <sup>c</sup> From steady-state surface tension experiments.

remains nearly constant for the lowest concentrations and then decreases linearly with increasing concentration, which suggests that the water surface is saturated by the copolymer. The value of  $C$  at the inflection point corresponds to the critical aggregation concentration (CAC). For each copolymer, a significant surface activity was observed for copolymer concentrations higher than 1 g/L, whereas dextran did not exhibit any surfactant property. However, one can observe in Figure 2 that  $\pi_{\text{CAC}}$  ( $\pi_{\text{CAC}} = \sigma_{\text{CAC}} - \sigma_0$ ,  $\sigma_0$  for pure water) varies from 10 to 15 mN/m depending on the considered copolymer. It is, however, difficult only with these results to interpret the observed differences in  $\pi_{\text{CAC}}$ : many parameters are involved in the surface activity of copolymers such as their backbone flexibility, the respective length of the hydrophilic and hydrophobic parts, and the graft content for graft copolymers.<sup>29</sup> Moreover, the adsorption of grafted amphiphilic copolymers at the air/water interface often is the result of a cooperative effect: the first hydrophobic graft adsorbed at this interface assists the migration of the neighbor graft carried by the same hydrophilic backbone. Finally, a copolymer layer is formed at the interface, with no possible exchange with the bulk phase because the copolymer is quite irreversibly adsorbed at the interface. It has already been reported that  $\pi_{\text{CAC}}$  generally increased with the graft number, whatever the graft length.<sup>11,29</sup>

The solubility of the Dex-*g*-PLA could be another critical factor influencing  $\pi_{\text{CAC}}$ . For example, in case of Dex29K-*g*-18PLA<sub>0.1K</sub>,  $\pi_{\text{CAC}}$  was 12 and 17 mN/m at 25 and 46 °C, respectively. Actually, the higher the temperature, the more soluble the copolymer, the more closely packed its organization and the higher its amount at the interface. Besides, no significant change in the CAC was observed from one copolymer to another. As usually in amphiphilic copolymers, it was relatively difficult to evaluate with high accuracy the lower inflection point corresponding to the CAC. These CAC values remain in the range 0.3–0.6 g/L (Table 2). Nevertheless, these experiments demonstrated that all water-soluble Dex-*g*-PLA exhibited noticeable surfactant properties.

A comparison with some other similar surfactants is rather difficult because of the lack of published papers dealing with amphiphilic grafted polysaccharide-based copolymers. Actually, many reports concern dextran modified with low hydrophobic chain such as phenoxy<sup>29</sup> or fatty acid esters.<sup>8</sup> For these copolymers, the surface pressure decrease ( $\pi_{\text{CAC}}$ ) is higher than that observed for Dex-*g*-PLA since it can reach 30 mN/m. Such a difference could be certainly explained by the nature of the side chains since alkyl or aromatic side groups are more hydrophobic than the PLA grafts. Anyway, it remains that one of the main advantages of the Dex-*g*-PLA is that they can be totally biodegraded in natural

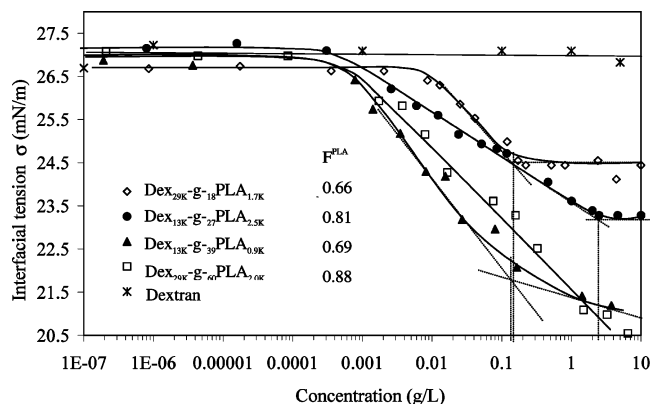


**Figure 3.** Variation of the interfacial tension ( $\sigma$ ) at the water/ $\text{CH}_2\text{Cl}_2$  interface as a function of the concentration of various Dex-*g*-PLA soluble in organic solvents.

metabolites. Moreover, the moderate surfactant activity observed for Dex-*g*-PLA<sub>m</sub> is generally sufficient to gain some stability in many processes where an emulsion is involved.

**Copolymers Soluble in Organic Solvents.** The technique used for this study was quite similar to the previous one but in this case, the copolymers were dissolved in dichloromethane and the steady-state interfacial water/dichloromethane tension was measured. As shown in Figure 3, each copolymer exhibits moderate surfactant properties. Depending on the compound, the interfacial tension reduction varies from 2.5 to 6 mN/m and increases with the number of grafts ( $\gamma$ ), whatever the dextran and PLA lengths. To explain such a behavior, one can assume that there is a cooperative effect at interface during the copolymer adsorption as in water-soluble copolymers. However, further investigations will be necessary to confirm this trend. In addition, a different behavior was observed for Dex<sub>13K</sub>-*g*-<sub>39</sub>PLA<sub>0.9K</sub> and Dex<sub>29K</sub>-*g*-<sub>60</sub>PLA<sub>2.0K</sub> compared to Dex<sub>29K</sub>-*g*-<sub>18</sub>PLA<sub>1.7K</sub> and Dex<sub>13K</sub>-*g*-<sub>27</sub>PLA<sub>2.5K</sub>. In fact, for the first ones no plateau of low interfacial tension was observed in the studied concentrations range  $<10$  g/L. As for the surface tension measurements, this phenomenon is not easy to interpret since many parameters change from one copolymer to another and studies with many other polymers will be necessary to establish relationship between the polymer molecular parameters and the interfacial properties.

As in the previous case, the CAC was difficult to evaluate precisely. Nevertheless, the CAC value seems to increase with the polylactide fraction in the copolymer ( $F^{\text{PLA}}$ ), that is, its hydrophobicity.

In conclusion, in each case (water-soluble compounds or not), the amphiphilic Dex-*g*-PLA showed ability to adsorb at interfaces and so revealed surfactant properties. It is thus possible to envisage their use as macromolecular surfactants in emulsions, in particular those employed for the formulation of PLA nanospheres by the specific emulsion/solvent evaporation procedure described elsewhere.<sup>30,31</sup> Indeed, Dex<sub>29K</sub>-*g*-<sub>14</sub>PLA<sub>0.2K</sub> was used as surfactant to stabilize a dichloromethane/water emulsion in such a process and nanoparticles with dextran at the interface were obtained with a mean diameter of 200 nm. Further surface analysis of these particles revealed lower value of zeta potential for these particles compared to uncovered PLA particles. This is due to the dextran layer at their surface masking the

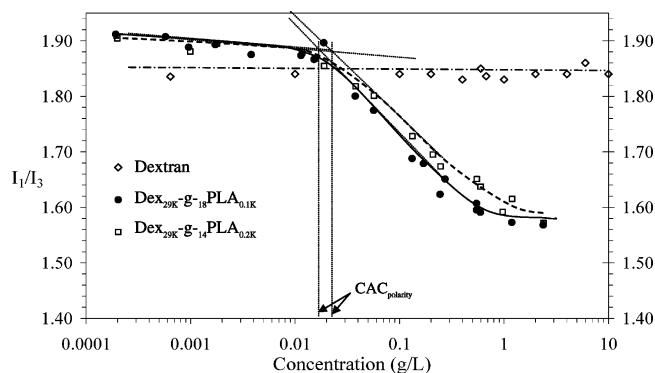


**Figure 4.** Variation of ( $I_1/I_3$ ) of the pyrene fluorescence as a function of the concentration of water-soluble Dex-*g*-PLA (water, 25 °C, [pyrene] =  $1 \times 10^{-6}$  mol/L,  $\lambda_{\text{ex}}$  = 330 nm).

carboxyl end groups of the PLA core. The thickness of the dextran layer was evaluated to about 30 nm.

**3.3 Fluorescence Measurements.** Depending on their solubility, the Dex-*g*-PLA<sub>m</sub> behavior was studied using external fluorescent probes either in aqueous or in toluene solutions.

**Water-Soluble Copolymers.** Water-soluble amphiphilic copolymers usually have the ability to generate hydrophobic microdomains in dilute aqueous solution by intra- or intermolecular associations between hydrophobic grafts. Various fluorescence probes can be used to characterize such an organization.<sup>32</sup> The fluorescence emission spectra of such probes depend on the solvent polarity, which is illustrated by either a change in band intensities ( $I$ ) or maximum emission wavelength ( $\lambda_{\text{max}}$ ) or in the fluorescence quantum yield ratio ( $\Phi_f/\Phi_0$ ).

Regarding pyrene, one of the most widespread probes, the ratio ( $I_1/I_3$ ) of the first and third band intensity at 372 and 383 nm, respectively, gives an appreciable indication of medium polarity surrounding it. The decrease in this ratio can be used to evidence hydrophobic microdomain formation<sup>32</sup> after a critical aggregation concentration we will name CAC<sub>polarity</sub>. For amphiphilic polymer concentrations higher than CAC<sub>polarity</sub>, ( $I_1/I_3$ ) reaches a constant value characteristic of the polarity of the hydrophobic microdomains wherein pyrene is included.

For the water-soluble Dex-*g*-PLA, ( $I_1/I_3$ ) decreases as a function of the copolymer concentration in water from 1.9 (value corresponding to the polarity of water) to a value below 1.6 (polarity of the hydrophobic microdomains), while no variation was observed in dextran (Figure 4). The final value below 1.6 was a little higher than that observed for an ethyl acetate medium.<sup>33</sup> Despite different structures, the behavior of the two studied water-soluble Dex-*g*-PLA was quite similar. The observed decrease of ( $I_1/I_3$ ) demonstrates the ability of these copolymers to organize in solution.

We carried out similar studies with another type of fluorescent probe, a molecular rotor, to confirm and complete these first observed results. As already reported,<sup>7,33,34</sup> a cinnamylidene molecular rotor such as 1,1-dicyano-(4'-*N,N*-dimethylaminophenyl)-1,3-butadiene (DMAC) can give other highly valuable information on the formation of hydrophobic microdomains, wherein DMAC is. The DMAC fluorescence emission spectrum varies with the polarity as well as with the viscosity of the rotor microenvironment. On one hand, when hydrophobic microdomains are formed,  $\lambda_{\text{max}}$  decreases with the microenvironment polarity,<sup>34</sup> which

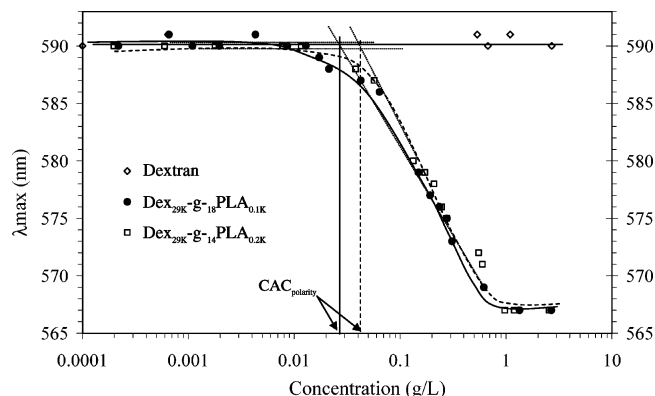


**Figure 5.** Variation of the emission maximum ( $\lambda_{\max}$ ) of DMAC as a function of the concentration of water-soluble Dex-*g*-PLA (water, 25 °C, [DMAC] =  $3.3 \times 10^{-6}$  mol/L,  $\lambda_{\text{ex}}$  = 493 nm).

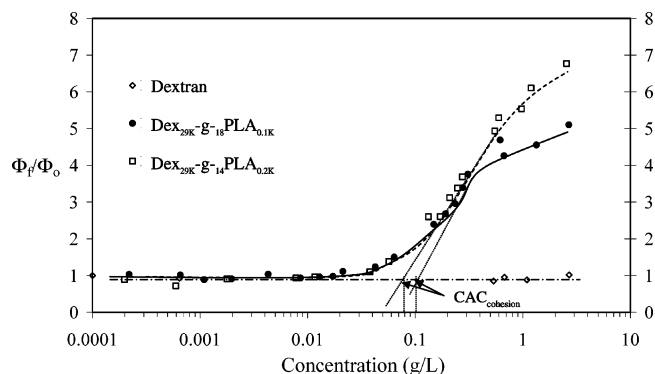


**Figure 6.** Variation of the fluorescence quantum yield ratio ( $\Phi_f/\Phi_0$ ) as a function of the concentration of water-soluble Dex-*g*-PLA (water, 25 °C, [DMAC] =  $3.3 \times 10^{-6}$  mol/L,  $\lambda_{\text{ex}}$  = 493 nm).

allows the determination of a critical aggregation concentration, called once again  $\text{CAC}_{\text{polarity}}$ . On the other hand, the fluorescence quantum yield ratio ( $\Phi_f/\Phi_0$ ) increases with the viscosity of the probe surroundings. This phenomenon is due to the decreasing mobility of the DMAC in viscous hydrophobic microdomains leading to a diminution of the nonradiative relaxation processes with a consequent increase of the fluorescence quantum yield ratio. This variation allows the determination of a critical aggregation concentration we will name  $\text{CAC}_{\text{cohesion}}$ . Both parameters ( $\lambda_{\max}$  and  $\Phi_f/\Phi_0$ ) were investigated, plotted as a function of the copolymer concentration, and compared to those of a dextran aqueous solution (Figures 5 and 6). For dextran solutions, the above-mentioned parameters did not change with polysaccharide concentration. In contrast, with the polylactide-grafted dextrans, these parameters showed a sharp decrease when the copolymer concentration increased, corresponding to the formation of hydrophobic microdomains. The final plateau value of each parameter indicated either the polarity or the viscosity inside these microdomains.

As shown in Figure 5, a weak variation of  $\text{CAC}_{\text{polarity}}$  was observed between the two studied copolymers and the final  $\lambda_{\max}$  reached 567 nm, which is characteristic of an acetone-like hydrophobic medium. However, in Figure 6, one can see that the viscosity inside the hydrophobic microdomains neighboring DMAC depends on the studied copolymer (a constant value of  $\Phi_f/\Phi_0$  was not obtained because of the limited solubility of the copolymer in water). The copolymer with the lowest number of grafts, Dex<sub>29K</sub>-*g*-13.5PLA<sub>0.2K</sub>, was able to form

more compact hydrophobic microdomains since the maximum fluorescence quantum ratio ( $\Phi_f/\Phi_0$ ) observed was higher than that of Dex<sub>29K</sub>-*g*-18PLA<sub>0.1K</sub> (for the same polarity). This result could result from different types of organization in solution, as already observed for other copolymers.<sup>34</sup>

From each parameter, two critical aggregation concentrations ( $\text{CAC}_{\text{polarity}}$  and  $\text{CAC}_{\text{cohesion}}$ ) could be determined from DMAC experiments, which corresponds to the beginning of the hydrophobic microdomains formation (Table 2). The  $\text{CAC}_{\text{polarity}}$  and  $\text{CAC}_{\text{cohesion}}$  values thus observed were different because they correspond to different phenomena, that is, polarity and viscosity of the microenvironment. These values have been compared:  $\text{CAC}_{\text{polarity}}$  obtained with pyrene or DMAC are different because these values depend on the used probes, which have different hydrophobic characters. Anyway, these values are between  $10^{-3}$  and  $10^{-1}$  mol/L (Table 2), in the same magnitude order as those previously reported with hydrophobized polysaccharides.<sup>7</sup> Moreover, one can observe that  $\text{CAC}_{\text{cohesion}}$  was always higher than  $\text{CAC}_{\text{polarity}}$  for each copolymer. According to previous studies,<sup>7</sup> the simple interaction of probes with these grafts could already decrease the probe polarity environment characterized by  $\text{CAC}_{\text{polarity}}$  before the effective formation of hydrophobic microdomains by aggregation of PLA graft, which was characterized by  $\text{CAC}_{\text{cohesion}}$ . Moreover, it was observed that the  $\text{CAC}_{\text{polarity}}$  obtained with pyrene is always smaller than that obtained with DMAC, which is related to the higher hydrophobicity of pyrene.

In conclusion, we proved with fluorescence spectroscopy measurements that water-soluble copolymers are able to form hydrophobic microdomains. As shown in Table 2,  $\text{CAC}_{\text{viscosity}}$  was always smaller than  $\text{CAC}$  determined by steady-state tension measurement, as observed for other amphiphilic polymers.<sup>35</sup> The difference between these values is related to the observed physicochemical phenomena: fluorescence spectroscopy gave information on the microscopic surrounding of the probe in solution, while tension measurements gave macroscopic information in relationship with the organization of the amphiphilic copolymer both at interface and in solution.

**Copolymers Soluble in Organic Solvents.** Similarly, the behavior of Dex-*g*-PLA soluble in toluene was investigated by fluorescence spectroscopy. Similar studies have been already reported in ionic or nonionic molecular surfactants but, to the best of our knowledge, no published report deals with modified polysaccharide or amphiphilic graft copolymers, though the organization of Pluronic was published recently.<sup>27</sup> As the addition of a small amount of water is usually essential to provoke reverse organizations, Dex-*g*-PLA was examined in an organic solvent/water system in the presence of a fluorescence water-soluble probe. Similarly to the work of Vasilescu et al.,<sup>27</sup> we used 1-anilinonaphthalene-8-sulfonic acid (ANS) and we chose the toluene/water system. The fluorescence emission spectrum of ANS depends on both polarity and viscosity of the probe microenvironment.<sup>36,37</sup> The wavelength corresponding to the maximum of the wide band of the ANS fluorescence emission ( $\lambda_{\max}$ ) increases with the polarity of the probe microenvironment, whereas the fluorescence quantum yield decreases. ANS molecule actually exists in two different conformations (Figure 1). In such a way, the global emission spectrum of ANS



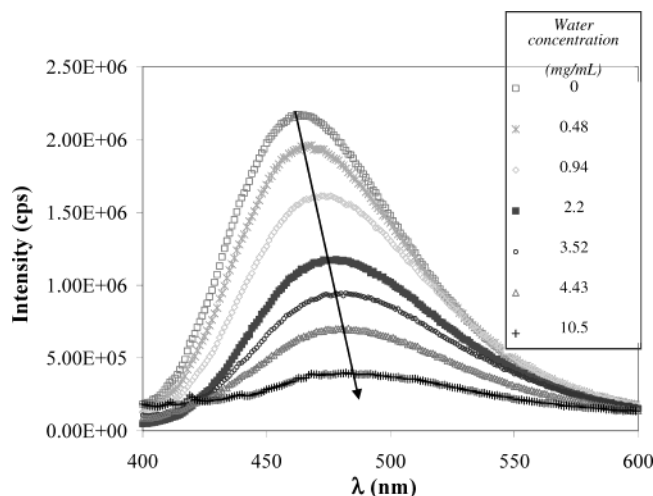


**Figure 7.** Fluorescence spectra of ANS in solution of Dex<sub>29K</sub>-*g*-<sub>18</sub>PLA<sub>1.7K</sub> in toluene/water systems as a function of water concentration at 25 °C. [Copolymer] = 5 g/L, [ANS] =  $3 \times 10^{-6}$  mol/L,  $\lambda_{\text{ex}}$  = 375 nm.

can be deconvoluted in two Gaussian bands, each one corresponding to one conformation.<sup>27</sup> Therefore, the wavelengths ( $\lambda_1$  and  $\lambda_2$ ) and the intensities ( $I_1$  and  $I_2$ ) corresponding to the maximum fluorescence emission for each band can be determined.  $\lambda_1$  and  $\lambda_2$  rise with the polarity of the ANS surrounding, whereas the intensity ratio  $R_F$  ( $R_F = I_1/I_2$ ) increases with both polarity and viscosity of the probe microenvironment.<sup>27</sup> The ratio and the position of these two bands depend on the microenvironment neighboring ANS. Thus,  $\lambda_{\text{max}}$  shifts from 466 nm in toluene to 555 nm<sup>27</sup> in water (Figure 7). The value of  $R_F$  reaches 1 in apolar medium and increases with the water concentration.

In case of Dex-*g*-PLA, ANS fluorescence emission spectra in the toluene/water systems exhibited the classical evolution ( $\lambda_{\text{max}}$  increased and  $I_{\text{max}}$  decreased with the increase of water concentration) corresponding to the increase in polarity in the ANS surrounding (Figure 7). No significant variation of both  $\lambda_{\text{max}}$  and  $R_F$  were observed in the absence of Dex-*g*-PLA, which proved that the difference in the probe surrounding was due to the copolymer and to its organization in the presence of water.

Moreover, a jump of  $\lambda_1$  and  $R_F$  parameters was observed for a certain amount of water for both studied copolymers as shown in Figure 8, whereas there was no significant change without copolymer. For a very little amount of water,  $R_F$  values are similar and higher than 1, with or without copolymer. In the presence of Dex-*g*-PLA,  $I_1$  and  $I_2$  decrease when the water concentration increases, affecting the second band to a greater extent, which results in an increase in  $R_F$ . The jump of both  $\lambda_1$  and  $R_F$  is thus assigned to a more polar and a more viscous surrounding of ANS, generated by the formation of hydrated microdomains. Thus, these phenomena clearly demonstrate the formation of a reverse organization of the studied copolymers, as soon as the proportion of water in toluene is sufficient (e.g., around 4 mg/mL for Dex<sub>13K</sub>-*g*-<sub>27</sub>PLA<sub>2.5K</sub>). Above a certain amount of water, these parameters ( $\lambda_1$  and  $R_F$ ) either reach a constant value or slowly increase. The reverse aggregation being already formed at this water amount, these limit values correspond to the polarity or the viscosity inside the organized microdomains.

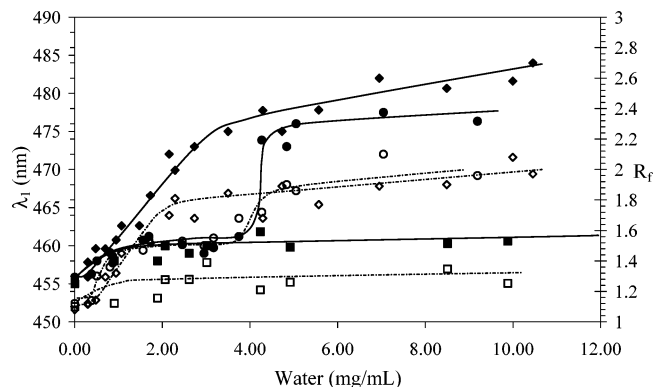


**Figure 8.** Variation of  $\lambda_1$  and  $R_F$  as a function of water concentration (25 °C, [Copolymer] = 5 g/L, [ANS] =  $3 \times 10^{-6}$  mol/L,  $\lambda_{\text{ex}}$  = 375 nm). For  $\lambda_1$  and  $R_F$  definitions, see the text. Open symbols are related to  $R_F$ , when closed ones are related to  $\lambda_1$ . Experiments were carried out with Dex<sub>29K</sub>-*g*-<sub>18</sub>PLA<sub>1.7K</sub> (◆), Dex<sub>13K</sub>-*g*-<sub>27</sub>PLA<sub>2.5K</sub> (●), or without copolymer (■).

The necessary amount of water needed to obtain the formation of final hydrated microdomains varies from one copolymer to another and increases with either the PLA weight fraction ( $F^{\text{PLA}}$ ) or the number of grafts in the copolymer (Table 1). However, further experiments with other Dex-*g*-PLA<sub>*m*</sub> copolymers will be necessary to precise the influence of these parameters.

If we try to compare our results with those obtained by Vasilescu et al.<sup>27</sup> with Pluronics in a xylene/water system, one can observe some differences, in particular, in  $R_F$  and in water amount necessary to form the hydrated microdomains, but it is clear that these two copolymers (Dex-*g*-PLA and Pluronics) present strong differences in chemical composition, hydrophilic/hydrophobic balance, and particularly architecture so that such a comparison is not obvious.

In conclusion, Dex-*g*-PLA showed a self-organization ability in solution, whatever their solubility. In water-soluble copolymers, hydrophobic microdomains are formed, whereas hydrated reverse microdomains take place for copolymers soluble in toluene with very small amounts of water. This organization ability can be paralleled with the surfactant properties of the copolymers, previously highlighted with the tension measurements. Nevertheless, it is difficult to make direct correlation between these two phenomena as one corresponds to an organization in solution, while the other depends on the competition between the organization in solution and the most probably irreversible adsorption at the interface.

## Conclusion

The controlled synthesis of amphiphilic polylactide-grafted dextran copolymers was achieved through a three-step strategy based on the "grafting from" method. In the first step, the dextran hydroxyl functions were partially protected by silylation. Polylactide grafts were then generated from the remaining hydroxyl groups by catalyzed ROP of D,L-lactide. The third step involved the silyl ether deprotection under very mild conditions. Owing to previous detailed studies,<sup>23–25</sup> all the synthesized glycopolymers possess very well defined architectures in terms of number and lengths of polyester grafts and polysaccharide backbone. The parameters of these copolymers vary in a broad range, especially concerning their PLA weight fraction. Depending on this fraction, copolymers are either water-soluble or soluble in organic solvents.

Whatever their solubility, all the synthesized copolymers showed noticeable surfactant properties. First of all, adsorption at the air/water or dichloromethane/water interfaces was evidenced by interfacial tension measurements. Fluorescence spectroscopy experiments also gave information about their self-organization in solution. Water-soluble copolymers were studied in the presence of two different probes (pyrene and DMAC) in water, while fluorescence experiments in toluene/water system were carried out with ANS in copolymers soluble in toluene. In both cases, the ability of the copolymers to generate organization in solution was demonstrated. Depending on their solubility, hydrophobic or hydrated microdomains were observed.

As a result, the design of new totally degradable dextran-based amphiphilic graft copolymers with well-defined macromolecular parameters was attainable. The surfactant properties of such glycopolymers could be useful in many environmentally friendly applications, especially in biomedical application requiring an interface stabilization during their process.

**Acknowledgment.** This work was supported by Tournesol Program n°00827WH for 2000 and 2001. The authors express their highest gratitude to Marie-Christine Grassiot (LCPM) for help in tension measurements. Finally, they are especially grateful to Dr Marie-Laure Viriot (DCPR) for advice in fluorescence studies. Ph.Dubois is much grateful to both Région Wallonne and Fonds Social Européen in the frame of Objectif 1-Hainaut: Materia Nova program and the Interuniversity Attraction Poles Program, Belgian Science Policy (IUAP, 5/03).

## References and Notes

- (1) Chen, J.; Jo, S.; Park, K. *Carbohydr. Polym.* **1995**, *28*, 69–76.
- (2) Pelletier, S.; Hubert, P.; Payan, E.; Marchal, P.; Choplin, L.; Dellacherie, E. *J. Biomed. Mater. Res.* **2001**, *54*, 102–108.
- (3) Qu, X.; Wirsén, A.; Albertsson, A. C. *Polymer* **2000**, *41*, 4589–4598.
- (4) Elvira, C.; Mano, J. F.; San Ramon, J.; Leis, R. L. *Biomaterials* **2002**, *23*, 1955–1966.
- (5) Akiyoshi, K.; Kang, E. C.; Kurumada, S.; Sunamoto, J.; Principi, T.; Winnik, F. M. *Macromolecules* **2000**, *33*, 3244–3249.
- (6) Miralles-Houzelle, M. C.; Hubert, P.; Dellacherie, E. *Langmuir* **2001**, *17*, 1384–1391.
- (7) Fischer, A.; Houzelle, M. C.; Hubert, P.; Axelos, M. A. V.; Geoffroy-Chapotot, C. G.; Carré, M. C.; Viriot, M. L.; Dellacherie, E. *Langmuir* **1998**, *14*, 4482–4488.
- (8) Bauer, K. H.; Reinhart, T.; Stenz, R. *Macromol. Symp.* **1997**, *120*, 39–45.
- (9) Marchant, R. E.; Rueggsegger, M.; Qiu, Y. In *Polysaccharides*; Dumitriu, S., Ed.; Marcel Dekker: New York, Basel, Hong-Kong, 1998; pp 851–886.
- (10) Zhang, T.; Marchant, R. E. *J. Colloid Interface Sci.* **1996**, *177*, 419–426.
- (11) Wollenweber, C.; Makievski, A. V.; Miller, R.; Daniels, R. *J. Colloid Interface Sci.* **2000**, *117*, 419–426.
- (12) Gref, R.; Rodrigues, J.; Couvreur, P. *Macromolecules* **2002**, *35*, 9861–9867.
- (13) Dubois, P.; Krishnan, M.; Narayan, R. *Polymer* **1999**, *40*, 3091–3100.
- (14) Cai, Q.; Wan, Y.; Jianzhong, B.; Wang, S. *Biomaterials* **2003**, *24*, 3555–3562.
- (15) Teramoto, Y.; Nishio, Y. *Polymer* **2003**, *44*, 2701–2709.
- (16) Ohya, Y.; Maruhashi, S.; Ouchi, T. *Macromolecules* **1998**, *31*, 4662–4665.
- (17) Ohya, Y.; Maruhashi, S.; Ouchi, T. *Macromol. Chem. Phys.* **1998**, *199*, 2017–2022.
- (18) Li, J.; Xie, W.; Cheng, M.; Nickol, R. G.; Wang, P. G. *Macromolecules* **1999**, *32*, 2789–2792.
- (19) Donabedian, D. H.; McCarthy, S. P. *Macromolecules* **1998**, *31*, 1032–1039.
- (20) Choi, E. J.; Kim, C. H.; Park, J. K. *Macromolecules* **1999**, *32*, 7402–7408.
- (21) Li, Y.; Volland, C.; Kissel, T. *Polymer* **1998**, *39*, 3087–3097.
- (22) Ydens, I.; Rutot, D.; Degee, P.; Six, J. L.; Dellacherie, E.; Dubois, P. *Macromolecules* **2000**, *33*, 6713–6721.
- (23) Nouvel, C.; Dubois, P.; Dellacherie, E.; Six, J. L. *J. Polym. Sci., Part A: Polym. Chem.* **2004**, *42*, 2577–2588.
- (24) Nouvel, C.; Ydens, I.; Degee, P.; Dubois, P.; Dellacherie, E.; Six, J. L. *Polymer* **2002**, *43*, 1735–1743.
- (25) Nouvel, C.; Dubois, P.; Dellacherie, E.; Six, J. L. *Biomacromolecules* **2003**, *4*, 1443–1450.
- (26) Harkins, W. D.; Jordan, H. F. *J. Am. Chem. Soc.* **1930**, *52*, 1751.
- (27) Vasilescu, M.; Caragheorgheopol, A.; Caldararu, H.; Bandula, R. *J. Phys. Chem. B* **1998**, *102*, 7740–7751.
- (28) Matsuoka, M.; Takao, M.; Kitao, T.; Fujiwara, T.; Nakatsu, K. *Mol. Cryst., Liq. Cryst.* **1990**, *182A*, 71.
- (29) Rouzes, C.; Durand, A.; Leonard, M.; Dellacherie, E. *J. Colloid Interface Sci.* **2002**, *253*, 217–223.
- (30) Rouzes, C.; Gref, R.; Leonard, M.; Delgado, A. D.; Dellacherie, E. *J. Biomed. Mater. Res.* **2000**, *50*, 557–565.
- (31) Chognot, D.; Six, J.-L.; Leonard, M.; Bonneaux, F.; Vigneron, C.; Dellacherie, E. *J. Colloid Interface Sci.* **2003**, *268*, 441–447.
- (32) Winnik, F. M.; Regismond, S. T. A. *Colloids Surf., A Physicochem. Eng. Aspect* **1996**, *118*, 1–39.
- (33) Sinquin, A.; Houzelle, M. C.; Hubert, P.; Choplin, L.; Viriot, M. L.; Dellacherie, E. *Langmuir* **1996**, *12*, 3779–3782.
- (34) Benjelloun, A.; Brembilla, A.; Lochon, P.; Adibnejad, M.; Viriot, M. L.; Carre, M. C. *Polymer* **1996**, *37*, 879–883.
- (35) Frochot, C.; Muller, C.; Brembilla, A.; Carre, M. C.; Lochon, P.; Viriot, M. L. *Int. J. Polym. Anal. Charact.* **2000**, *6*, 109–122.
- (36) Kosower, E. M.; Tanizawa, K. *Chem. Phys. Lett.* **1972**, *16*, 419.
- (37) Penzer, G. R. *Eur. J. Biochem.* **1972**, *25*, 218–228.

MA049857X